Proceedings of the International Symposium on Physics of Materials (ISPMA13)

Influence of Pre-Compression on Tensile Behaviour in Wrought Mg–Zn–Ce Alloy Studied by the Acoustic Emission Technique

P. Dobroň[a,*], D. Drozdenko[a], J. Bohlen[b], S. Yi[b], D. Letzig[b] and F. Chmelík[a]

[a]Charles University in Prague, Department of Physics of Materials, Ke Karlovu 5, 12116 Prague 2, Czech Republic

[b]Helmholtz-Zentrum Geesthacht, Zentrum für Material- und Küstenforschung GmbH, Max-Planck-Str. 1, D21502 Geesthacht, Germany

Wrought Mg–Zn–Ce alloy (ZE10) has been pre-compressed and subsequently subjected to tensile loading. Due to a fibre texture of the samples, the level of pre-compression stress significantly influences the subsequent tensile behaviour. The acoustic emission technique was used for monitoring active deformation mechanisms during mechanical testing. The obtained acoustic emission results are correlated to the stress-time curves and the differences in the acoustic emission count rate were used to reveal changes in underlying deformation mechanisms. Firstly, a compression-tension cycle was monitored by the acoustic emission technique. Then, the samples were deformed to specific points on the stress-time curve, where acoustic emission exhibits strong changes in the activity. The following microstructure analysis of the samples, deformed to different strain-levels, by using electron back scattered diffraction method brought a detailed insight into active deformation mechanisms. Twinning during the pre-compression was followed by detwinning during the tensile loading. Two consecutive acoustic emission peaks, which appeared at larger strains, are explained by interplay of detwinning and dislocation slip and a nucleation of compression twins, respectively.

DOI: 10.12693/APhysPolA.128.790

PACS: 81.05.Bx, 62.20.M–, 61.05.J–, 81.70.Bt, 43.40.Le

1. Introduction

Mechanical properties of wrought Mg alloys are significantly influenced, besides of hexagonal closed packed (hcp) crystallographic lattice of Mg, by strong initial texture. Generally, plastic deformation in Mg alloys at room temperature (RT) is realized by dislocation slip and twinning, where the elongation of the hcp unit cell along the *c*-axis is accommodated by $\{10{-}20\}$ twins and the contraction by $\{10{-}11\}$ or $\{10{-}13\}$ twins, unless the critical resolved shear stress (CRSS) for non-basal slip systems is reached [1]. Thus, twinning is a key deformation mechanism in Mg alloys, especially during cyclic loading, when the occurrence of the twinning-detwinning process induces important changes in the deformation behaviour. The twinning-detwinning behaviour can be frequently seen during fatigue tests of wrought Mg alloys [2–4]. Cáceres et al. [5] have studied the pseudoelastic behaviour in a cast AZ91 magnesium alloy during tensile cyclic loading-unloading. The hysteresis curves were attributed to the cyclic motion of the twin boundary. The strong basal texture of extruded Mg alloys, having basal planes almost parallel to the extrusion direction (ED), favour the occurrence of $\{10{-}20\}$ twins during compression along ED [1].

Tensile loading of the pre-compressed Mg alloy leads to disappearing of $\{10{-}20\}$ twins due to an easier activation of the detwinning process than the twinning one [6]. The influence of detwinning on mechanical properties is commonly studied by scanning electron microscopy [7–12] or diffraction methods with applying the visco-plastic self consistent (VPSC) polycrystal model [13, 14]. Li and Enoki [15, 16] have applied acoustic emission (AE) method for a study of anelastic recovery in pure Mg and AZ31 magnesium alloy during a cyclic compression test. Bohlen et al. [17] have shown that compression-tension cyclic tests in an AZ31 magnesium alloy with various pre-compression stress lead to significant changes in the AE response. In that work a preferential formation of twins occurs in large long grains that have been identified as unrecrystallized remain of the extrusion microstructure development. The aim of the present work is to specifically exclude such a feature of the microstructure and use an extruded profile with a fully recrystallized and homogeneous grain structure.

It has been shown in previous work [18] that ZE10 is a good candidate for this research. Therefore, in this paper the tensile behaviour of a pre-compressed ZE10 magnesium alloy is studied by a combination of AE and electron back scattering diffraction (EBSD) technique in order to characterise the active deformation mechanisms. Hence, the *in situ* AE technique provides real time information about collective dislocation dynamics and the nucleation of twins and the *post mortem* EBSD method characterises corresponding changes in the microstructure.

2. Experimental procedure

The ZE10 (Mg + 1.3 wt% Zn + 0.1 wt% Ce) magnesium alloy cast billet with average grain size of (449±26) μm was indirectly extruded at 300 °C with extrusion speed of 10 m/min (profile exit speed) in order

*corresponding author; e-mail: dobronp@karlov.mff.cuni.cz

to produce a round bar with a diameter of 17 mm. The extrusion ratio was 1:30.

Specimens with a diameter of 8 mm and a gauge length of 15 mm were machined from the round bar parallel to the extrusion direction (ED). Deformation tests were carried out at room temperature using a universal testing machine Zwick® Z50 at a constant strain rate of 10^{-3} s^{-1}. First of all, compression test until fracture was performed in order to select pre-compression stress, at which a lot of twins will have been created in the alloy; however, most of grains favourable oriented for twinning are still not fully twinned. Pre-compression stress was set to 150 MPa and it was followed by tensile loading until fracture. Additionally, mechanical tests were repeated and stopped at distinct points in order to carry out microstructure analysis.

AE during deformation tests was monitored by computer-controlled PCI-2 device (Physical Acoustic Corporation) using a piezoelectric transducer with a flat response between 100 and 600 kHz and a preamplifier giving a gain of 40 dB. The threshold level of the detection was set to 26 dB (above the peak noise level).

EBSD was used to analyze the microstructure of the samples on their electropolished longitudinal sections with a field emission gun scanning electron microscope (Zeiss Ultra 55, EDAX/TSL EBSD system and Hikari detector). Special attention was paid to the type and distribution of the twins. The EBSD measurements were performed with an accelerating voltage of 15 kV and a step size of 0.3 μm. A software "TSL OIM Analysis" was used to analyse the results. The identification of point-to-point-misorientations was used to identify grain- and specific twin boundaries. A twin area analysis is carried out manually by selecting identified twins.

3. Experimental results

The ZE10 alloy has almost homogeneous microstructure with an average grain size of (21±2) μm and basal texture is represented by strong orientations along the arc between the ⟨10−10⟩ — and the ⟨11−20⟩ — poles (Fig. 1). The stress, the AE signal record and the AE count rate dependence on time is presented in Fig. 2. The deformation test starts with pre-compression up to 150 MPa (plotted as positive values) and is subsequently followed by tensile loading (plotted as negative values) till the fracture. The compressive yield strength (CYS) is achieved at (81±1) MPa and as the plastic deformation proceeds, the stress–time curve has an increasing slope. After pre-compression, the tensile deformation curve exhibits S-shape, which is typical for compression test of extruded Mg alloys. The deformation curve is correlated to the concurrent AE measurement trough measuring time. The AE signal is very strong during pre-compression, especially in the region of the compressive yield point, whereas during tensile loading, smaller AE amplitudes linked with a detection of inflection points on the deformation curve are observed (Fig. 2(top)). Using the threshold level detection of the AE signals, the

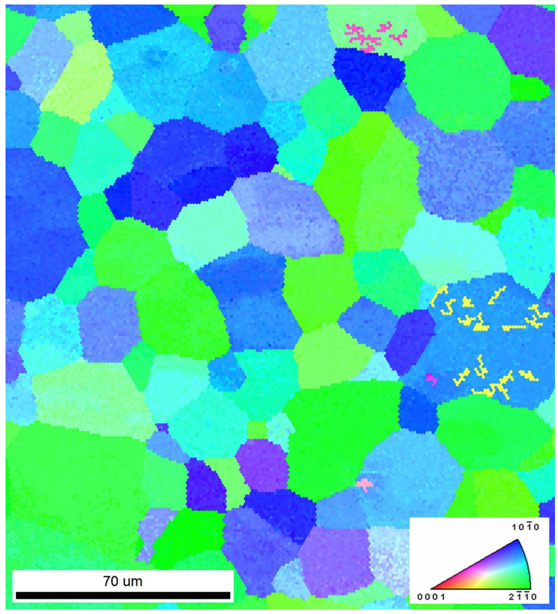

Fig. 1. Orientation map of the initial microstructure of the extruded ZE10 magnesium alloy.

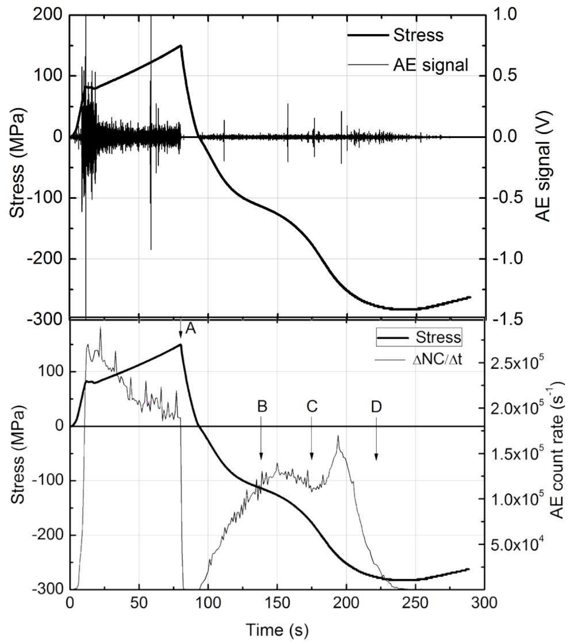

Fig. 2. Stress, AE signal and AE count rate *vs.* time curves for the extruded ZE10 magnesium alloy.

AE count rate ($\Delta N_C/\Delta t$ — number of counts per second, as defined by ASTM E1067 [19]) was determined (Fig. 2(bottom)). Such parametrization offers important information about collective dynamic processes which occur during plastic deformation. The AE count rate exhibits a maximum at CYS. Unloading from 150 MPa to zero does not produce any AE signals. During tensile loading, two maxima in the AE count rate are present.

The EBSD analysis was performed on the samples which were stressed to different stages of deformation (in as received condition — zero stress — Fig. 1; marked

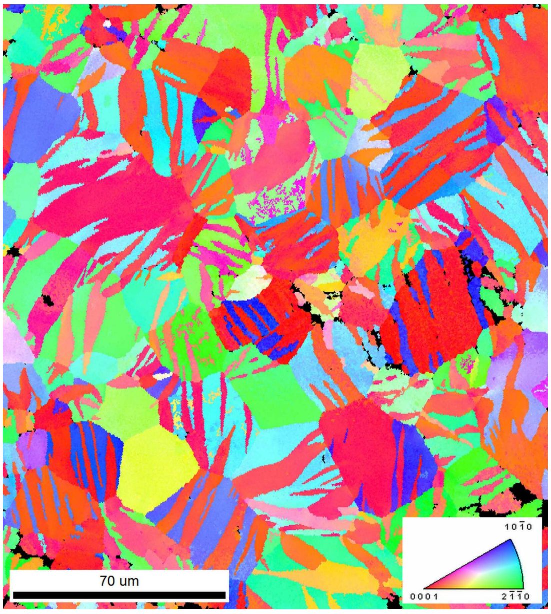

Fig. 3. Orientation map of the extruded round bar after compression to 150 MPa (position A in Fig. 2).

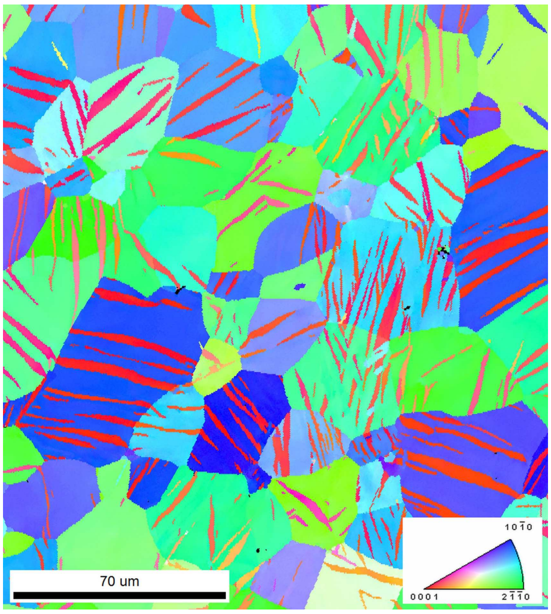

Fig. 4. Orientation map of the extruded round bar after compression to 150 MPa and tension to 130 MPa (position B in Fig. 2).

as A, B, C and D position in Fig. 2(bottom)) in order to study the twinning activity (significant changes in the AE activity). According to the character of the deformation curve and the corresponding AE response, presented in Fig. 2, tensile stress values of 130 MPa (B), 180 MPa (C), and 275 MPa (D) were chosen. The microstructure of pre-compression samples contains a lot of twins (Fig. 3). The inverse pole figure (IPF) exhibits a strong $\langle 0001 \rangle$ pole intensity to not present in the as received condition, which indicates the activity of tensile twins.

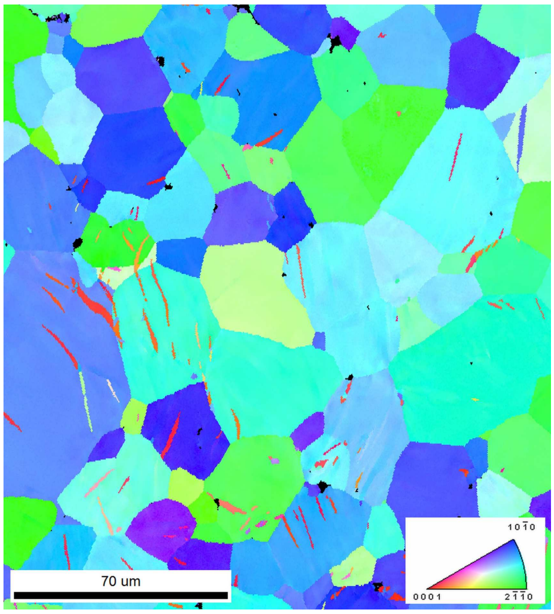

Fig. 5. Orientation map of the extruded round bar after compression to 150 MPa and tension to 180 MPa (position C in Fig. 2).

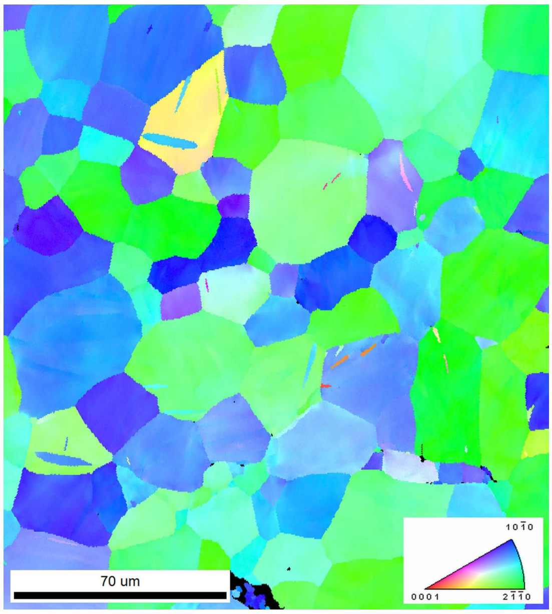

Fig. 6. Orientation map of the extruded round bar after compression to 150 MPa and tension to 275 MPa (position D in Fig. 2).

Furthermore, the EBSD analysis shows the presence of $\{10-20\}$ "extension"- twins only.

The orientation maps for samples, which have been pre-compressed and subsequently loaded in tension to the specific stress, can be seen in Figs. 4–6. During tensile loading to 130 MPa (Fig. 4), twins are smaller and the $\langle 0001 \rangle$ pole intensity is also reduced (strong intensity in $\langle 10-10 \rangle$- or $\langle 11-20 \rangle$-orientation) by comparison with the pre-compressed sample. The misorientation angle distribution shows a maximum for 86.4°, which corresponds with the activity of tensile twins. The orientation map for the sample loaded in tension to 180 MPa (C position in Fig. 2) can be seen in Fig. 5. Microstructure contains a small number of twins and in the IPF, the $\langle 0001 \rangle$ pole intensity is not present any more. In the sample loaded in tension to 275 MPa (D position in Fig. 2), small amount of compression twins were observed (Fig. 6).

4. Discussion

As can be seen in Fig. 1, the extruded ZE10 magnesium alloy exhibits a strong basal texture, where the basal planes are almost parallel to ED favouring the activation of $\{10-20\}$ twins, if compression stress is applied. Plastic deformation during pre-compression starts in grains favourably oriented for $\langle a \rangle$ dislocation glide in the basal and prismatic plane [20]. Thus, collective movement of dislocations produces detectable AE signals even before achieving the macroscopic yield point (YP). Similar results can be found e.g. in [21–23] for wrought Mg alloys with a strong deformation texture.

To retain the compatibility of plastic deformation during the compression test, with respect to very high CRSS for the activation of non-basal slip systems [1, 20], the occurrence of twins is required. From the EBSD results (Fig. 3), it can be seen that a lot of grains contain $\{11-20\}$ "extension"-twins which are assigned to the angle of 86.4°. Thus, the plastic deformation proceeds by basal slip in grains reoriented due to twinning and, after reaching CRSS for activation of non-basal slip systems, it proceeds also by $\langle c + a \rangle$ dislocation slip. A relative low CYS and an intense AE signal at macroscopic YP is connected with collective dislocation processes and a nucleation of twins. It was presented in [24, 25] that the twin nucleation is an excellent source of AE, in contrary to twin thickening, where no AE signal occurs. The AE signals, observed after YP, are produced by strong dynamic processes whose AE activity is yet not reduced by strain hardening. In Ref. [26], Dobron et al. have studied the grain size effect on twinning in extruded AZ31 during compression test and by using AE and EBSD. They have shown that twinning starts in larger grains and as plastic deformation proceeds, twins also occur in smaller grains. Therefore, the high AE activity persisting during strain hardening and a large amount of $\{10-12\}$ "extension"-twins in pre-compressed microstructure (Fig. 3) can be explained by "continuous" nucleation of twins during the test.

Unloading from the compression stress of 150 MPa (position A in Fig. 2) to zero stress does not produce any AE signals which is in accordance with the fact that lower deformation stress cannot re-open already closed dislocation sources (the Kaiser effect [27]). On the contrary, tensile loading re-opens dislocation sources and subsequent collective dislocation movement produces detectable AE signals. The activity of the AE signal during tensile loading is lower than during the pre-compression (Fig. 2) due to higher dislocation density which reduces the flight distance and the free length of moving dislocations. Furthermore, the detwinning process, which occurs during tensile loading, does not contribute to AE activity [17].

The evidence on the detwinning process can be found in Fig. 4, where microstructure of the samples pre-compressed to 150 MPa and subsequently tensile loaded to 130 MPa (position B in Fig. 2) exhibits obvious shrinkage of twins compared to microstructure in Fig. 3. Also, the reduction of the basal $\langle 0001 \rangle$ pole intensity can be ascribed to this fact. The microstructure of the sample loaded to 180 MPa (position C in Fig. 2) contains only small amount of tensile twins, which means that the detwinning process continues after achieving the position B on the deformation curve (Fig. 2). The AE count rate increases from the beginning of tensile loading due to detwinning, where detwinned grains have a favourite orientation for basal slip. Two opposite processes influence the AE activity during tensile loading. Namely, the increasing number of detwinned grains supports the AE activity through the rise in the flight distance and the free length of moving dislocations and, on the contrary, the increasing dislocation density means a stronger barrier for their movement and, therefore, reduces the AE signal. The first AE maximum at 150 s (Fig. 2) indicates the point where hardening overcomes the detwinning (softening) effect. The second AE maximum is related to the nucleation of compression twins which is supported by the EBSD measurement (Fig. 6). Only nucleation of twins can produce AE signals, which are not yet reduced by strain hardening. Similar influence of nucleation of twins on the AE activity was observed in [26].

5. Conclusions

The strong basal texture of the extruded ZE10 magnesium alloy favours the activation of tensile $\{10-12\}$ $\langle 10\bar{1}\bar{1} \rangle$ twins during pre-compression of the samples. The subsequent tensile loading leads to the detwinning process which has a similar influence on the deformation behaviour as twinning (S-shape of the deformation curve). The AE measurement at very low tensile stresses confirms the fact that the shrinkage of twins cannot produce a detectable AE signal. Furthermore, intensive shrinkage at higher tensile stresses, which was observed by the EBSD method, obviously does not significantly contribute to the AE response. Thus, the AE activity during tensile loading is the result of collective dislocation processes. The strong increase in AE count rate at very high tensile stresses can be explained by the activation of the compression twins.

Acknowledgments

This work received support from the Czech Science Foundation under the grant 13–19812S. The work of P.D. is a part of activities of the Charles University Research Center "Physics of Condensed Matter and Functional Materials". D.D. is grateful for financial support from the Grant Agency of Charles University under grant No. 1882314 and also for the grant SVV-2015-260213.

References

[1] P.G. Partridge, *Metall. Rev.* **118**, 169 (1967).

[2] L. Wu, A. Jain, D.W. Brown, G.M. Stoica, S.R. Agnew, B. Clausen, D.E. Fielden, P.K. Liaw, *Acta Mater.* **56**, 688 (2008).

[3] S.M. Yin, F. Yang, X.M. Yang, S.D. Wu, S.X. Li, G.Y. Li, *Mater. Sci. Eng. A* **494**, 397 (2008).

[4] W. Wu, S.Y. Lee, A.M. Paradowska, Y. Gao, P.K. Liaw, *Mater. Sci. Eng. A* **556**, 278 (2012).

[5] C.H. Cáceres, T. Sumitomo, M. Veidt, *Acta Mater.* **51**, 6211 (2003).

[6] X.Y. Lou, M. Li, R.K. Boger, S.R. Agnew, R.H. Wagoner, *Int. J. Plasticity* **23**, 44 (2008).

[7] T. Hama, N. Kitamura, H. Takuda, *Mater. Sci. Eng. A* **583**, 232 (2013).

[8] S.H. Park, J.H. Lee, Y.H. Huh, S.G. Hong, *Scr. Mater.* **69**, 797 (2013).

[9] A. Chapuis, Y. Xin, X. Zhou, Q. Liu, *Mater. Sci. Eng. A* **612**, 431 (2014).

[10] L. Wang, G. Huang, Q. Quan, P. Bassani, E. Mostaed, M. Vedani, F. Pan, *Mater. Des.* **63**, 177 (2014).

[11] Y. Xin, X. Zhou, L. Lv, Q. Liu, *Mater. Sci. Eng. A* **606**, 81 (2014).

[12] Y.P. Li, Y. Cui, H. Bian, S. Sun, N. Tang, Y. Chen, B. Liu, Y. Koizumi, A. Chiba, *Sci. Technol. Adv. Mater.* **15**, 035003 (2014).

[13] H. Wang, P.D. Wu, C.N. Tomé, J. Wang, *Mater. Sci. Eng. A* **555**, 93 (2012).

[14] G. Proust, C.N. Tomé, A. Jain, S.R. Agnew, *Int. J. Plasticity* **25**, 861 (2009).

[15] Y.P. Li, M. Enoki, *Mater. Trans.* **48**, 2343 (2007).

[16] Y.P. Li, M. Enoki, *Mater. Trans.* **49**, 1800 (2008).

[17] J. Bohlen, P. Dobroň, L. Nascimento, K. Parfenenko, F. Chmelík, D. Letzig, *Acta Phys. Pol. A* **122**, 444 (2012).

[18] P. Dobroň, F. Chmelík, K. Parfenenko, D. Letzig, J. Bohlen, *Acta Phys. Pol. A* **122**, 593 (2012).

[19] ASTM E1067/E1067-M-11, 2011, *Standard Practice for Acoustic Emission Examination of Fiberglass Reinforced Plastic Resin (FRP) Tanks/Vessels.*

[20] M.R. Barnett, *Mater. Sci. Eng. A* **464**, 1 (2007).

[21] P. Dobroň, J. Bohlen, F. Chmelík, P. Lukáč, D. Letzig, K.U. Kainer, **Mater. Sci. Eng. A 462**, 307 (2007).

[22] M. Janeček, R. Král, P. Dobroň, F. Chmelík, V. Šupík, F. Holländer, *Mater. Sci. Eng. A* **462**, 311 (2007).

[23] J. Čapek, K. Máthis, B. Clausen, J. Stráská, P. Beran, P. Lukáš, *Mater. Sci. Eng. A* **602**, 25 (2014).

[24] C.R. Heiple, S.H. Carpenter, *J. Acoust. Emission* **6**, 215 (1987).

[25] J.P. Toronchuk, *Mater. Eval.* **35**, 51 (1977).

[26] P. Dobroň, F. Chmelík, S. Yi, K. Parfenenko, D. Letzig, J. Bohlen, *Scr. Mater.* **65**, 424 (2011).

[27] J. Kaiser, Ph.D. Thesis, TU München, 1950.